10.1071/CH15163_AC

Australian Journal of Chemistry 2016, 69(2), 220-229

Supplementary Material

Synthesis and Characterization of Mesoporous Tin Oxide Functionalized Reduced Graphene Oxide Nanoplatelets for Ultrasensitive Determination of Guaiacol in Red Wines

Tian Gan[A,B] *Zhaoxia Shi,*[A] *Kaili Wang,*[A] *Junyong Sun,*[A] *Zhen Lv,*[A] *and Yanming Liu*[A]

[A]College of Chemistry and Chemical Engineering, Xinyang Normal University, Xinyang 464000, PR China

[B]Corresponding author. Email: gantianxynu@163.com.

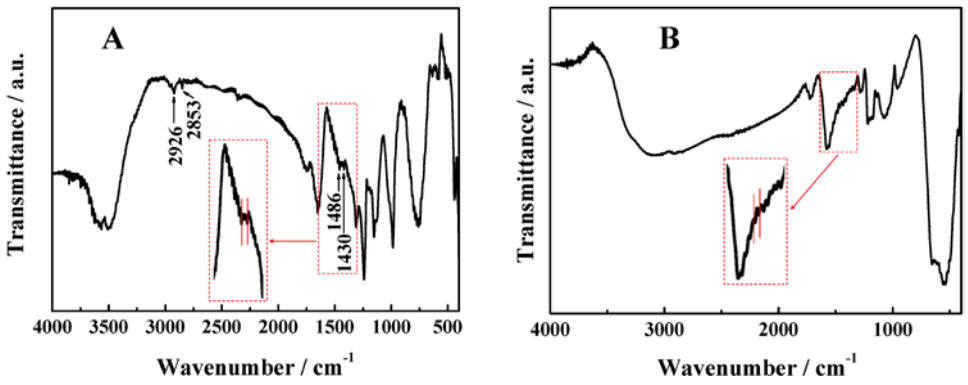

Fig. S1 FTIR spectra of SnO_2–rGO prepared with (A) and without (B) the assistance of CTAB.

The FTIR spectrum of SnO_2–rGO prepared with the assistance of CTAB exhibits bands for asymmetric and symmetric C–H scissoring vibrations of CH_3–N^+ at 1486 and 1430 cm^{-1}, respectively. The absorption peaks at 2853 and 2926 cm^{-1} are related to the stretching vibration of alkyl C–H bonds (–CH_3 and –CH_2) (Fig. S1A). However, all of the signature bands are not visible in the FTIR spectrum of the SnO_2–rGO prepared without the assistance of CTAB (Fig. S1B). This is the evidence of CTAB.

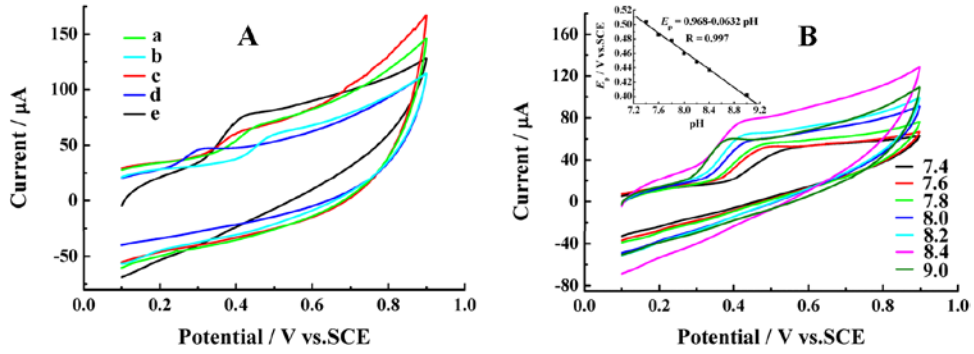

Fig. S2 (A) CV curves of 50 μM guaiacol at SnO_2–rGO/CPE in pH 7.4 disodium hydrogen phosphate–citric acid (a), pH 5.8 acetic acid–sodium acetate (b), pH 8.6 disodium hydrogen phosphate–sodium dihydrogen phosphate (c), pH 9.90 sodium carbonate–sodium bicarbonate (d) and pH 8.4 boric acid–borax (e). (B) CV curves of 50 μM guaiacol at SnO_2–rGO/CPE in pH 7.4–9.0 boric acid–borax buffer. The inset shows the plot of E_p vs. pH.

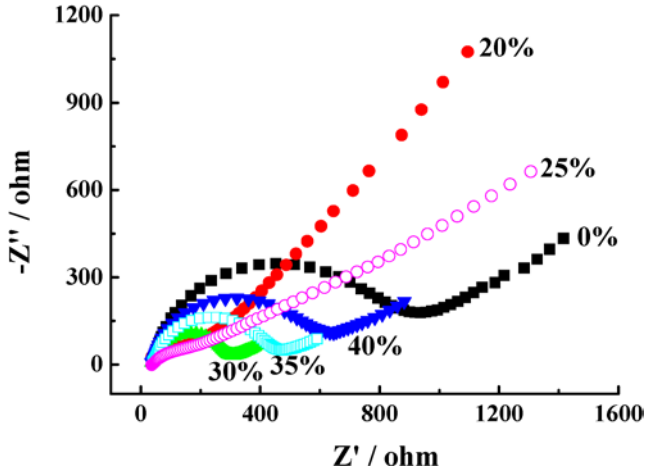

Fig. S3 Electrochemical impedance spectra obtained on CPE modified with different content of SnO_2–rGO in 0.1 M KCl containing 5 mM $[Fe(CN)_6]^{3-/4-}$. Frequency range is from 0.1 to 10^5 Hz with perturbation amplitude of 5 mV.

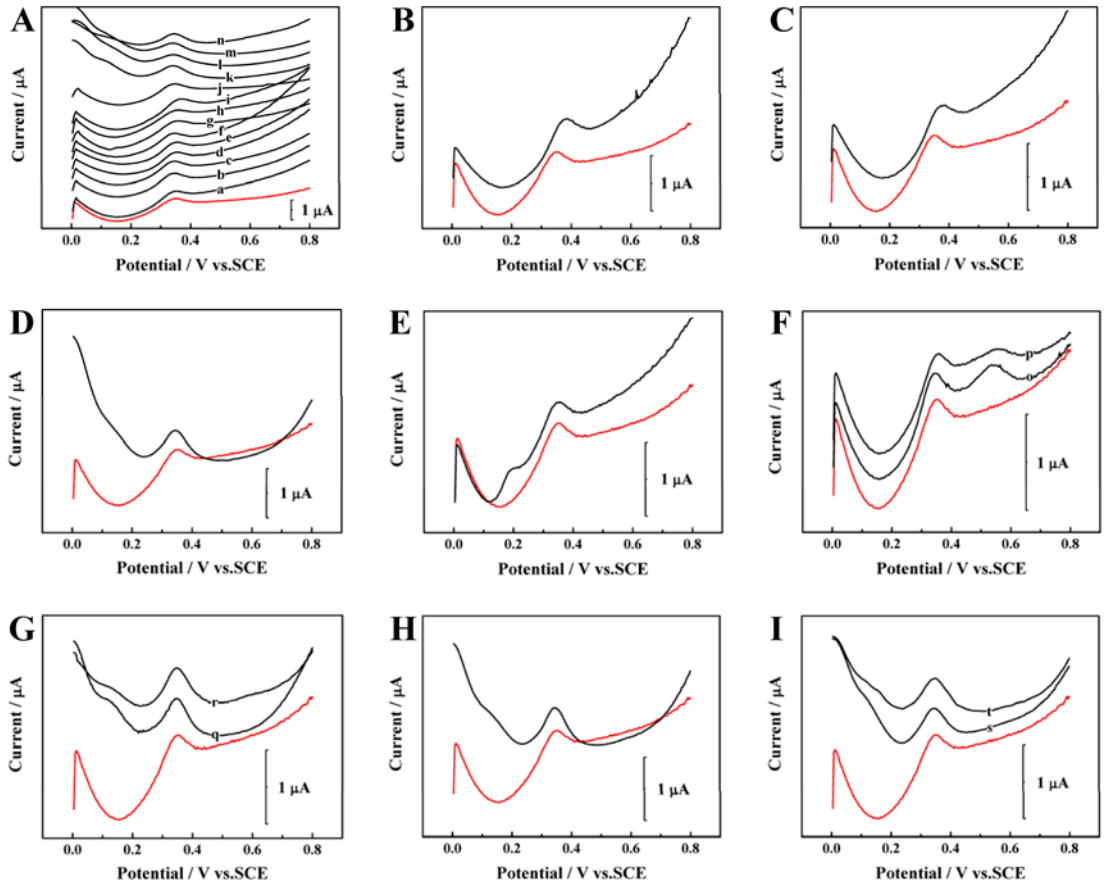

Fig. S4 (A) DPV curves of 5.0 μM guaiacol in pH 8.4 boric acid–borax buffer containing 10 mM Zn^{2+} (a), K^{+} (b), NO^{3-} (c), Cu^{2+} (d), SO_4^{2-} (e), Mg^{2+} (f), Na^{+} (g), Cl^{-} (h), Ca^{2+} (i), glucose (j), sucrose (k), tartaric acid (l), aminocaproic acid (m) or citric acid (n). (B) DPV curves of 5.0 μM guaiacol in pH 8.4 boric acid–borax buffer containing 7.5 mM Fe^{3+}. (C) DPV curves of 5.0 μM guaiacol in pH 8.4 boric acid–borax buffer containing 5 mM Al^{3+}. (D) DPV curves of 5.0 μM guaiacol in pH 8.4 boric acid–borax buffer containing 3.9 mM ascorbic acid. (E) DPV curves of 5.0 μM guaiacol in pH 8.4 boric acid–borax buffer containing 0.5 mM uric acid. (F) DPV curves of 5.0 μM guaiacol in pH 8.4 boric acid–borax buffer containing 100 μM vanillin (o) or maltol (p). (G) DPV curves of 5.0 μM guaiacol in pH 8.4 boric acid–borax buffer containing 1 mM cresol (q) or syringol (r). (H) DPV curves of 5.0 μM guaiacol in pH 8.4 boric acid–borax buffer containing 250 μM phenol. (I) DPV

curves of 5.0 μM guaiacol in pH 8.4 boric acid–borax buffer containing 125 μM 4–ethylguaiacol (s) or 4–methylguaiacol (t). The red curves in these figures correspond to the DPV response of 5.0 μM guaiacol in pH 8.4 boric acid–borax buffer.